

RESEARCH ARTICLE SUMMARY

EPIGENETICS

Design principles of 3D epigenetic memory systems

Jeremy A. Owen, Dino Osmanović, Leonid Mirny*

INTRODUCTION: During development, our cells establish different identities—nerve, muscle, blood, and so on—which can remain stable even as the cells grow and divide. This stability is a form of epigenetic memory. Evidence suggests that this memory is partly held within chromatin itself, probably in patterns of chemical modifications of DNA and histones known as “epigenetic marks.” But individual marks are highly dynamic, being placed and removed by many mechanisms, and are partly lost when DNA is replicated. How can patterns of dynamic marks be a seat of stable memory?

RATIONALE: In the transcriptionally silent heterochromatin, the loss of histone marks is counterbalanced by “reader-writer” enzymes that effectively spread marks between neighboring nucleosomes. However, in simple models, this mechanism cannot maintain mark patterns; if mark spreading is strong enough to restore a partially erased pattern, marks tend to spread uncontrollably. An account of epigenetic memory must invoke ingredients beyond simple mark spreading.

A tantalizing possibility is that this missing element is the three-dimensional (3D) folding of the genome. Recent experiments suggest that marks might spread not just along the chromatin polymer but also in three dimensions between nucleosomes near each other in space. Additionally, regions carrying heterochromatic marks are known to attract each other, making heterochromatin segregate from other regions

and forming a denser nuclear compartment. Mechanisms for epigenetic memory could rely on this interplay between 3D compartmentalization and mark dynamics.

RESULTS: We developed a simple theoretical model of the dynamics of chromatin and its marks through the cell cycle. Over a single cell generation, we found that if marks spread in 3D, they sharply localize to dense chromatin regions. In fact, our model of mark dynamics is precisely analogous to a susceptible-infected-susceptible (SIS) epidemic model on a network; mark localization to the dense compartment is akin to an epidemic becoming endemic in densely populated areas while vanishing elsewhere.

However, over successive cell generations, as chromatin refolds according to the dynamic marks, we still see an all-or-none tendency for marks to spread everywhere or to be lost globally, destroying any epigenetic memory. We found that one more ingredient is needed: the limitation of reader-writer enzymes relative to their histone substrates. This very plausible but often neglected element completely changes model behavior, yielding a memory of mark patterns stable for hundreds of cell generations.

Our findings are insensitive to variations in model assumptions—for example, to the precise way loss of marks occurs—as long as three ingredients are present. First, there must be a considerable density difference between chromatin compartments. Second, a reader-writer enzyme must be able to spread marks in 3D.

And third, critically, those enzymes must be limited in abundance. We propose that the presence of these elements amounts to a basic design principle for epigenetic memory systems that exploit 3D genome structure for their function.

We find that our model provides a unified account of many observations, ranging from classic phenomena such as position-effect variegation to recent studies of the dynamics of mark recovery after replication. We can also make a number of predictions, particularly about single-cell epigenetic heterogeneity, that emerging techniques may be able to test.

CONCLUSION: Our work reveals a mechanism by which a coupling between 3D folding of the genome and mark dynamics could help cells remember their identities. Intuitively, the mechanism relies on the encoding of memory in different forms in different phases of the cell cycle. In interphase, memory is held in the 3D structure of the genome, whereas in mitosis, when the 3D structure is being totally reorganized, memory is held in the sequence of marks.

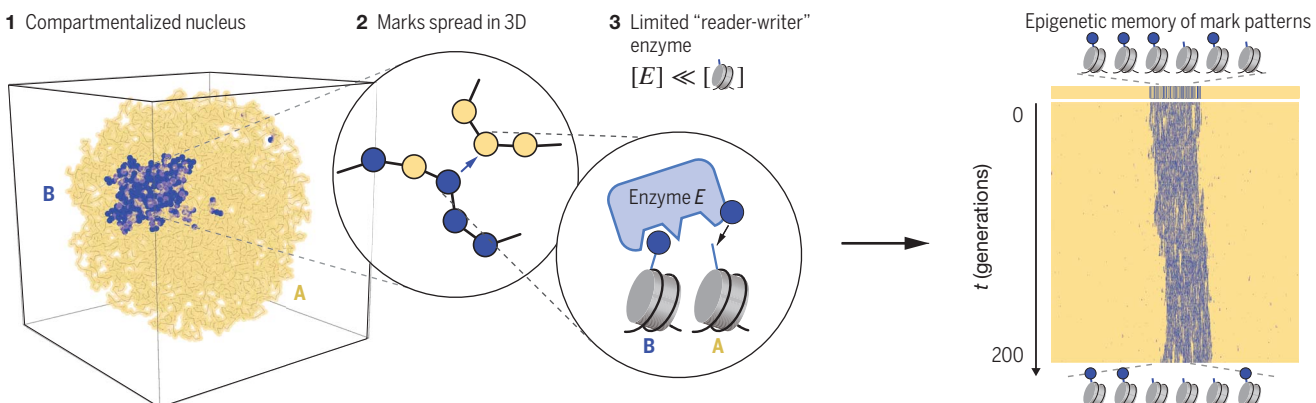
The encoding of a mark pattern could also be thought of as the “learning rule” of an associative memory in a Hopfield network, where connections between marked regions are established by folding them together (“mark together, park together”). In this analogy, the mark dynamics are like the “update rule” that allows recovery of a stored memory. We should keep in mind the possibility that epigenetic systems are capable not just of memory but also of more sophisticated information processing. ■

The list of author affiliations is available in the full article online.

*Corresponding author. Email: leonid@mit.edu

Cite this article as J. A. Owen et al., *Science* 382, eadg3053 (2023). DOI: 10.1126/science.adg3053

S READ THE FULL ARTICLE AT
<https://doi.org/10.1126/science.adg3053>



Design principles of 3D epigenetic memory. (Left) Our model of chromatin and its dynamics through the cell cycle reveals three key elements for stable epigenetic memory (right).

RESEARCH ARTICLE

EPIGENETICS

Design principles of 3D epigenetic memory systems

Jeremy A. Owen^{1†}, Dino Osmanović², Leonid Mirny^{1*}

Cells remember their identities, in part, by using epigenetic marks—chemical modifications placed along the genome. How can mark patterns remain stable over cell generations despite their constant erosion by replication and other processes? We developed a theoretical model that reveals that three-dimensional (3D) genome organization can stabilize epigenetic memory as long as (i) there is a large density difference between chromatin compartments, (ii) modifying “reader-writer” enzymes spread marks in three dimensions, and (iii) the enzymes are limited in abundance relative to their histone substrates. Analogous to an associative memory that encodes memory in neuronal connectivity, mark patterns are encoded in a 3D network of chromosomal contacts. Our model provides a unified account of diverse observations and reveals a key role of 3D genome organization in epigenetic memory.

Remembering gene expression states—that is, which genes are “on” or “off”—is a remarkable capability of living cells. It is well established that this “epigenetic” memory can be stably encoded in the abundances of freely diffusing transcription factors (TFs) that regulate each other’s synthesis (1–3). But in eukaryotes, such as ourselves, in addition to TF-based memory, there is evidence that memory can be held locally to the genes, in the chromatin (4–7). It has been suggested that a seat of this chromatin-based epigenetic memory could be the chemical modifications (marks) of the DNA-bound histones, which vary across the genome in patterns correlated with gene expression. However, chromatin and its marks are subject to large disruptions through the cell cycle, and it is not clear what is required to make stable memories out of mark patterns. In this study, we identified three qualitative elements that together are sufficient for stable epigenetic memory. Our minimal theoretical model incorporating these elements unites a battery of classic observations ascribed to epigenetic memory of heterochromatin, makes predictions that emerging experimental techniques can test, and suggests a functional role for a hallmark of nuclear organization: its three-dimensional (3D) compartmentalization.

Heterochromatin—the transcriptionally silent, denser nuclear compartment—is rich in particular histone marks, especially the lysine trimethylations H3K9me3 and H3K27me3. These marks are made by so-called reader-writer enzymes (8, 9), which can bind marked histones allosterically, stimulating their marking activity on neighboring histones, effectively

spreading marks between neighbors. Marked histones can be retained locally when the replication fork passes (10, 11), but they are (by necessity) diluted in the process by newly synthesized, unmarked histones. The combination of these two features is highly suggestive of a stable memory system, in which local mark spreading accurately restores mark patterns after their partial erasure at replication. However, simple mathematical models (12, 13) of this mechanism reveal a basic instability: If mark spreading is strong enough to restore a partially erased pattern, marks also spread ectopically to the rest of the chromosome.

Recent experiments suggest that reader-writer enzymes may be able to spread histone marks in three dimensions (9, 14, 15), that is, between histones that are nearby in space because of how chromatin is folded, not just in one dimension along the chromatin polymer. Because histone marks also contribute to the spatial compartmentalization of the genome, this raises the tantalizing possibility of a bidirectional coupling between the 3D folding of chromatin and the marks on the chromatin polymer (16–19). Could this help stabilize memory? Recent theoretical work (19–22) has explored some consequences of this putative coupling, but generally these studies have difficulty achieving a self-sustaining memory of mark patterns. An understanding of the qualitative conditions required for chromatin-based epigenetic memory is yet to emerge.

Model

In search of design principles for epigenetic memory, we developed and studied a simple biophysical model in which memory is held autonomously in mark patterns. In many prior models, mark patterns are sustained by external reinforcement—for example, by nucleation sites or genomic bookmarks (12, 13, 23) that recruit modifying enzymes—or by a static 3D contact structure (24). But a pattern determined

by external influences is not itself a seat of memory, and so we excluded such elements from our model.

We modeled chromatin as a long polymer of 10^4 monomers that is confined within a sphere (Fig. 1A). This could represent, in a coarse-grained manner, all the chromatin in the nucleus, or just a chromosomal region of 2 Mb (10^4 nucleosomes). Monomers in the polymer can be in one of two states, A or B, with B monomers representing marked, heterochromatic regions and A monomers representing unmarked, euchromatic ones. To represent the “stickiness” of heterochromatin (25–28), B monomers experience a short-range attraction (fig. S14) to one another of magnitude α , which leads B monomers to spatially segregate from the A monomers, forming a denser compartment.

To model the 3D spreading of marks (Fig. 1B), we supposed that A monomers turn into B monomers at a rate $S n_B$, where n_B is the number of neighboring B monomers within a 3D interaction radius, r_c (1.5 times the diameter of a monomer), and S is the spreading rate. B monomers turn back into A monomers at a constant rate L , uniformly at all sites, representing in aggregate the loss of marked histones owing to the activity of demodifying enzymes (e.g., demethylases), histone exchange, and replicative dilution. Our core results proved insensitive to precisely how the loss of marks is modeled (fig. S2).

To represent the cell cycle (Fig. 1C), we ran our model in two alternating phases. During “interphase,” we assumed that the chromatin is frozen in place while marks are spread and lost, reaching a steady state. By contrast, in “mitosis,” we assumed that marks remain unchanged while the chromatin polymer is compacted into a condensed state. Then, to establish a new interphase state, we allowed the polymer to expand subject to interactions between marked regions, naturally leading to compartmentalization (Materials and methods). We called each round of polymer dynamics followed by mark dynamics one “cell generation.” Our assumptions about the dynamics in each phase reflect experimental observations. In interphase, the gross 3D organization of chromatin is quite stable (29), whereas some marks can turn over completely on a timescale of minutes to hours (30, 31), a time over which chromatin loci may displace by just ~0.2 to 0.4 μm (32). By contrast, in mitosis, repressive marks appear to remain stable (33, 34) even while chromatin undergoes dramatic refolding. Several factors may account for this stability of marks, including inhibition of modifying enzymes by mitotic phosphorylation of the H3 tail (35, 36), decreased accessibility of mitotic chromatin, and the short duration of mitosis. Later in the study, we loosened the assumptions we made about the phases (figs. S3 and S4).

¹Department of Physics, Massachusetts Institute of Technology, Cambridge, MA, USA. ²Department of Mechanical and Aeronautical Engineering, UCLA, Los Angeles, CA, USA.

*Corresponding author. Email: leonid@mit.edu

†Present address: Department of Chemistry, Princeton University, Princeton, NJ, USA.

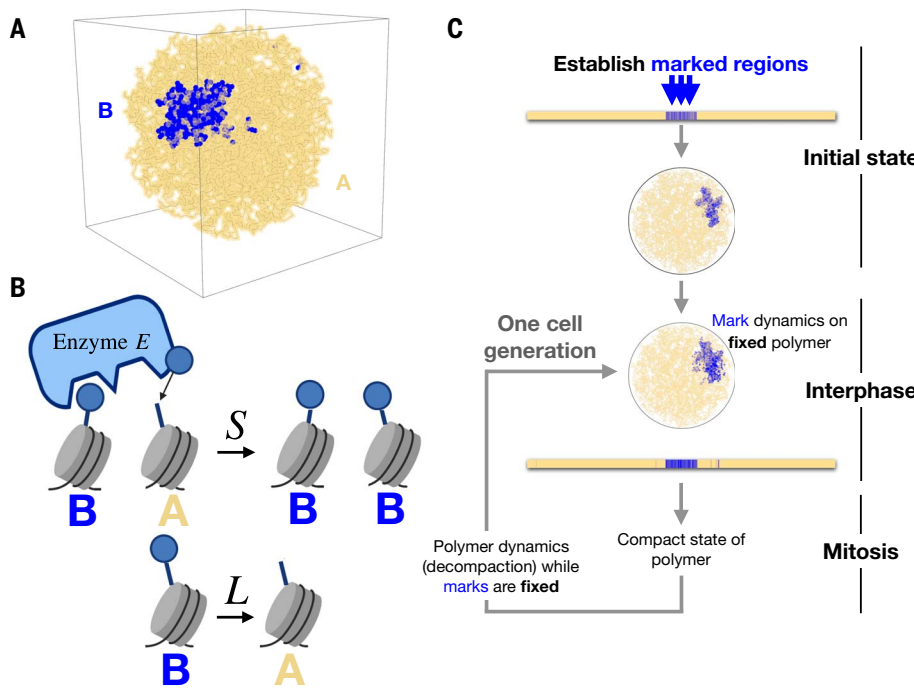


Fig. 1. Model of mark and chromatin dynamics. (A) Chromatin in the nucleus modeled as a spherically confined copolymer with monomers of two types, A (pale yellow) and B (blue), representing a varying pattern of histone marks. Monomers of type B, which represent regions bearing heterochromatic marks, self-attract. (B) Marks spread to 3D neighbors at rate S and are lost everywhere uniformly at rate L . (C) The overall dynamics of our model consist of alternating phases of polymer dynamics and mark dynamics, representing the cell cycle.

In our simulations, we set an initial pattern of A and B monomer identities before the first interphase and allowed it to evolve over one or many cell generations. If, at later times, the pattern resembles the initial pattern, and would do so for several possible initial patterns, then the system can be said to exhibit memory.

Results

Marks localize to dense regions providing stable memory for one cell generation

Over a single cell generation, we found that there is an extremely good memory of mark patterns. The steady state of the mark dynamics reached in the interphase closely resembles the initial mark pattern used to fold the polymer (Fig. 2, A and B). The steady-state pattern can recover after large perturbations, such as a complete randomization of the pattern (every monomer is randomly set to A or B) (Fig. 2A) or wholesale erasure of half of the pattern (Fig. 2B). The reason for the recovery of the pattern is that spreading marks tend to localize to dense regions; the remaining marks spread in 3D and restore the marks in the spatially dense compartment that was formed by the originally marked regions. It is as if the mark pattern has been “memorized” in the 3D configuration of the polymer.

An analogy to epidemic spreading can help us understand the localization of marks to dense regions quantitatively. The mark dynamics of

our model are identical to a susceptible-infected-susceptible (SIS) epidemic model on a network (37). The monomers of our polymer are like individuals whose “social” contact network (Fig. 2D) is defined by the polymer configuration, and the marked state is like the infected state. The infection, like marks, spreads at rate S , and infected individuals recover (lose marks) at rate L . A key parameter for epidemic spreading dynamics is the average number of neighbors, d , of an individual (monomer). Roughly, there is an “epidemic threshold,” $1/d$, such that if S/L is below $1/d$, the infection will die out.

Returning to our model with a dense and diffuse compartment, with average numbers of neighbors d_+ and d_- , respectively, this suggests that when S/L lies in the range

$$\frac{1}{d_+} \leq \frac{S}{L} \leq \frac{1}{d_-}$$

there should be sharp localization of marks to the dense compartment, with very few marks in the diffuse compartment (a more detailed discussion is provided in the supplementary text). Intuitively, this condition says that the system must be above the epidemic threshold in the dense region and below it in the diffuse region. Consistently, simulations (Fig. 2C) show localization of marks in an even broader range of S/L . As the strength of self-attraction, α , increases, the difference

in the densities grows (Fig. 2C, inset), further broadening this range. The analogy to epidemic spreading shows quantitatively how the density difference between the compartments underlies the sharp localization of marks to the dense compartment, providing robust recovery of the initial mark pattern within one cell generation.

Memory is lost over multiple cell generations

However, over multiple generations (Fig. 3), something very different happens. Sweeping through the parameter space of our model (Fig. 3B), what we found is an unstable, all-or-none behavior. When S/L is greater than a critical value, $\lambda_c(\alpha)$ (which depends on α), an initially marked region grows uncontrollably until it covers the entire polymer. When S/L is less than $\lambda_c(\alpha)$, marks are instead lost globally. In both cases, memory of the initial state is lost within a few generations. When there is strong self-attraction and S/L is fine-tuned to very near $\lambda_c(\alpha)$, memory lasts longer, but even then, there is a clear tendency to uncontrolled spread or global loss of marks. The same basic instability is apparent in the closely related model of Sandholtz *et al.* (21), who found that fine-tuning of parameters was required to achieve just five generations of mark-pattern memory. Taken together, 3D spread of marks, even when coupled with 3D genome folding through the self-attraction of marks, is not enough to provide lasting epigenetic memory.

Enzyme limitation stabilizes epigenetic memory

However, so far we have neglected a key biological fact, often omitted in biophysical models of mark dynamics. Marks do not spread by themselves; spreading requires the action of a reader-writer enzyme, which in the nucleus is likely to be limited relative to its histone substrates. Estimates of the abundances of the histone methyltransferases PRC2 and SETB1 (38–40), for example, suggest that they are hundreds to thousands of times less abundant than nucleosomes, which number in the tens of millions. To account for the limitation of the reader-writer enzymes, we introduced a Michaelis-Menten-type scheme (41, 42) in which A-B pairs that are within the interaction radius act as the substrate (Fig. 3F). Remarkably, we found that adding enzyme limitation to our model stabilizes the memory of the initial mark pattern (Fig. 3, D and E) for hundreds of cell generations and over a broad range of parameters.

The effect of enzyme limitation is to replace the spreading rate, S , by an effective spreading rate, S_{eff} , that depends on the number of A-B pairs, N_{AB} (supplementary text)

$$S_{\text{eff}} = \begin{cases} S & \text{if } N_{AB} < E_T \\ \frac{SE_T}{N_{AB}} & \text{if } N_{AB} \geq E_T \end{cases}$$

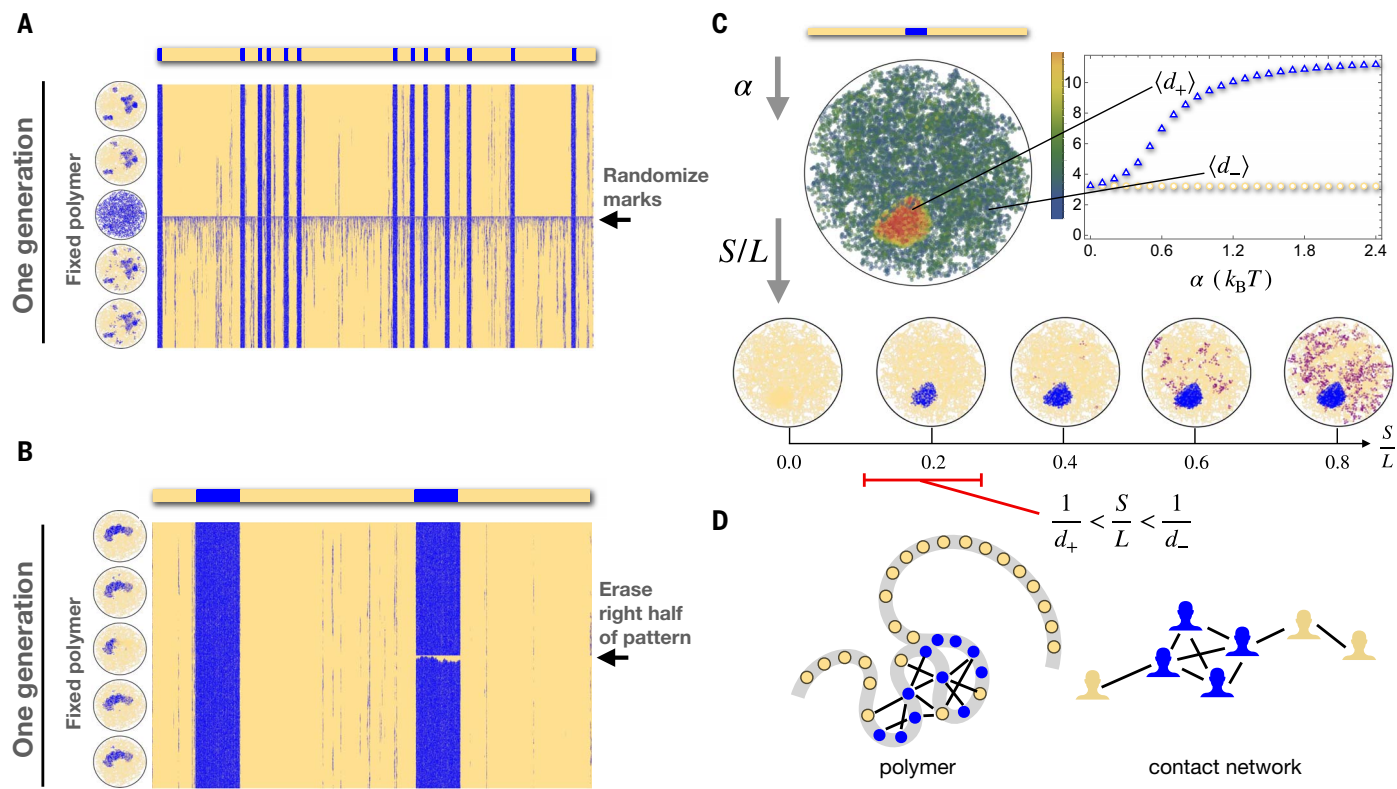


Fig. 2. Spreading marks sharply localize to dense regions. (A) Mark dynamics, with $S/L = 0.5$, over a single cell generation, on a fixed polymer folded according to an initial pattern, with $\alpha = 2.4 k_B T$ (where k_B is the Boltzmann constant and T is the temperature). Time advances from top to bottom. (Left) Inset circles show snapshots of the polymer configuration (2D projection) over time. (B) As in (A), with a different initial pattern and perturbation. (C) (Top) When the polymer folds, marked regions tend to be denser (red) than unmarked ones (green) because of the self-attraction of marks [density is quantified by the number of

monomer neighbors (color bar)]. The plot shows the average number of monomer neighbors in each compartment as a function of the strength of B-B self-attraction, α . (Bottom) In turn, when marks evolve according to their dynamics of spreading and loss, they tend to localize in dense regions for a range of S/L values. (D) An analogy to epidemic spreading, in which marked monomers are equivalent to infected people, predicts correctly that this localization will occur at least in the red interval, whose width is set by the number of neighbors in each region.

where E_T is the total amount of enzyme. Intuitively, the enzyme sets a maximum global modification rate: the “ V_{\max} ” of the enzyme, which equals SE_T . In those cases in which previously, marks spread uncontrollably across the whole polymer, now the total number of marks is set by the balance of V_{\max} and L to be $N_B = SE_T/L$. This fixing of the number of marks is sufficient to yield a stable memory of the mark pattern—for example, of the position of a marked domain (Fig. 3D and fig. S1). Stability of the mark pattern is also seen when loss occurs purely by replicational dilution (modeled as random loss of half the marks) once every cell cycle period, T_{div} , instead of at a constant loss rate, L (fig. S2). The stable memory is seen across a broad range of parameters as long as self-attraction is strong enough (Fig. 3E), and it works without external reinforcement or fine-tuning, as required by other models.

Design principles and model phenomenology

To summarize our findings so far, we have found a memory system that depends on three key ingredients, all characteristic of heterochromatin: (i) strong self-attraction of marked regions,

leading to nuclear compartmentalization and densification of marked regions; (ii) 3D spread of marks; and (iii) limitation of the reader-writer enzyme relative to its substrates. We propose that the presence of these elements together amounts to a basic design principle for epigenetic memory systems that exploit 3D genome structure for their function. Our results suggest that heterochromatin may be dense not necessarily to sterically exclude transcriptional machinery [heterochromatin is likely highly permeable to polymerase-size particles (43)] but rather as a way to maintain the memory of heterochromatin.

A rich observable phenomenology follows directly from these elements, providing strong support for our model, as well as many predictions to be tested by emerging experimental modalities.

The number of marks scales linearly with the enzyme concentration

First and most basically, our model relates the abundance of a mark to the activity (S) and concentration (E_T) of a reader-writer enzyme that makes it; in particular, we found a broad

regime in which the number of marks is linear in both of these quantities: $N_B = SE_T/L$. This prediction is at least consistent with the measured effects of EZH2 inhibition (44) and activating mutations (45, 46) on H3K27me3 levels (supplementary text), although a definitive test of linearity will require careful quantitation of both sides of the equation. Perhaps more unexpectedly, our model reveals that sometimes changing the concentration of an enzyme is different than uniformly changing its activity. This could shed light on mechanistic puzzles, such as the question of how the oncogenic mutant H3K27M histone reduces H3K27me3: Does it sequester limited PRC2 (effectively reducing E_T) (47), or does it persistently reduce its activity (e.g., S) after transient contact (38)? Our model predicts that varying E_T should change the number of marks smoothly, whereas reducing S/L below a critical value can cause a sharp, global loss of marks (fig. S5).

Stable domains remain only partly marked

Second, our model predicts that only about half of the monomers in marked regions are marked. As S/L or E_T is varied, the stable mark domains

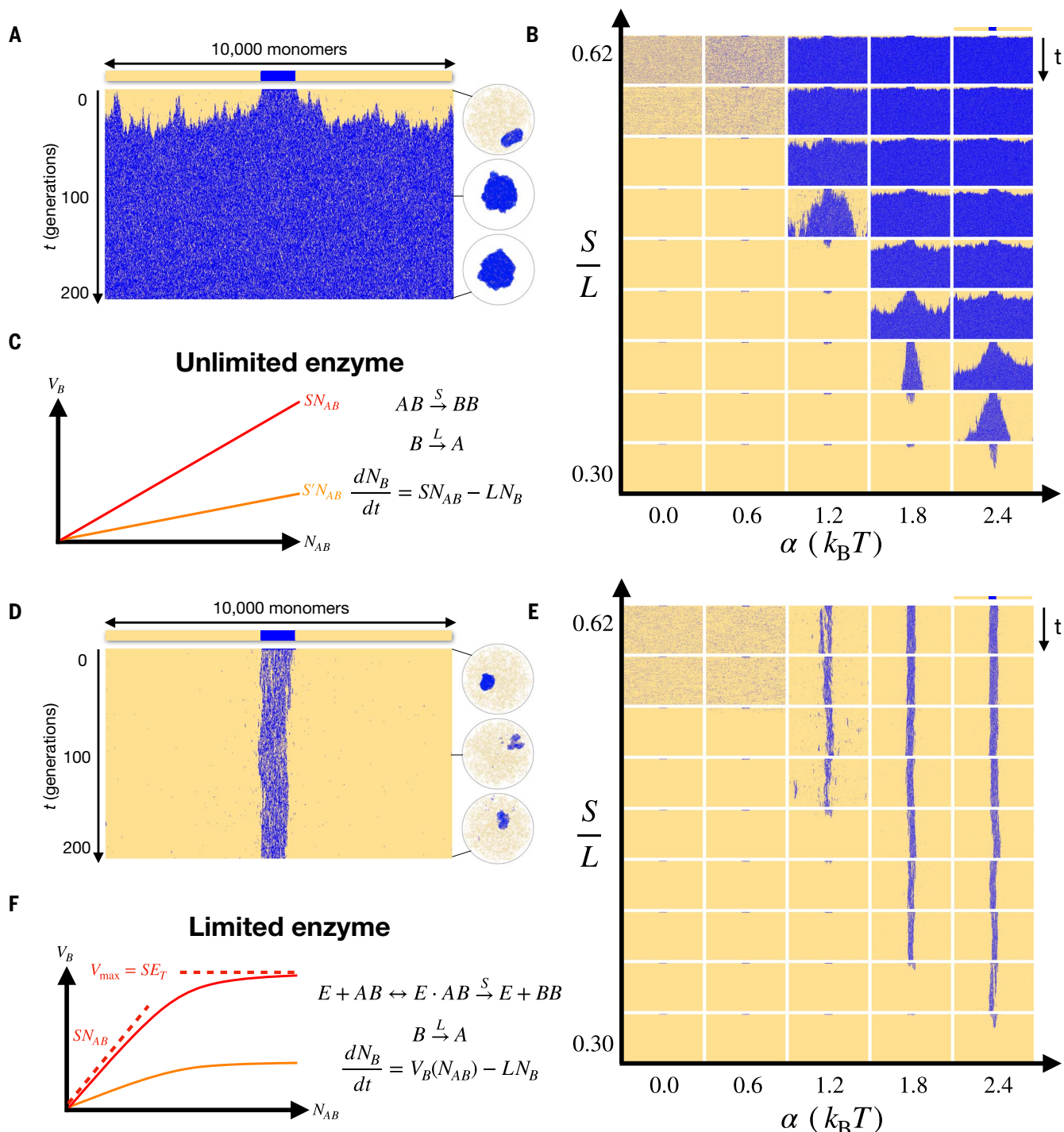


Fig. 3. Limited enzyme stabilizes memory over multiple generations.

(A) Time evolution of a mark pattern, with unlimited enzyme, over 200 generations ($\alpha = 2.4 k_B T$, $S/L = 0.42$), starting from an initial pattern consisting of a single domain of 1000 marked monomers. Inset circles show snapshots in time of the polymer configuration. For this choice of parameter, marks spread everywhere and the polymer collapses. (B) Time evolution of the mark pattern, with unlimited enzyme,

as a function of α and S/L . There is no stable memory. (C) With unlimited enzyme, the global marking rate in the nucleus, V_B , is proportional to the number N_{AB} of A-B pairs. (D and E) Just as in (A) and (B), but with limited enzyme, $E_T = 1000$. Stable memory is achieved for hundreds of generations, over a broad range of parameters. (F) With limited enzyme, V_B is proportional to N_{AB} when it is small, but then saturates at the value $V_{\max} = SE_T$, preventing uncontrolled spreading of marks.

(Fig. 3E) arising in the limited enzyme regime vary in length, but the fraction of monomers within the domain that are marked remains roughly constant, around 0.55 (fig. S6A). This “semimarking” phenomenon is consistent with

several experimental results. Semimarking leads to a density difference of two- to threefold between compartments (fig. S6B), which is consistent with observed differences between heterochromatic and euchromatic regions in the

nucleus (48). Semimarked domains also fold into irregular structures (fig. S6B)—as recently observed by super-resolution microscopy targeting Polycomb-repressed *Hox* genes (49)—instead of spheres, as would fully marked domains.

Additionally, semimarking explains the counterintuitive findings of Alabert *et al.* (50) showing that certain histone marks require several cell generations to be fully established on new histones after replicational dilution and that old histones keep getting marked; our model naturally reproduces these observations (fig. S7).

Mark redistribution and error correction

Third, our model predicts a coupling between distant genomic regions that is mediated by the titration of the limited enzyme. The plainest consequence of this is that if marks are lost somewhere, they tend to be gained elsewhere. In capturing this, our model agrees with the numerous observations of such titration effects in epigenetic systems (51–53). As one illustration of this, we show that our model (fig. S8) can emulate the findings of Kraft *et al.* (15), which demonstrated that genomic deletion of PRC2 nucleation sites can cause loss of H3K27me3 local to the deletion but gain of the mark elsewhere.

We found that this “mark redistribution” has a natural directionality to it: Marks tend to flow from smaller domains to larger domains. A pattern consisting of multiple, noncontiguous mark domains can be remembered for hundreds of generations (Fig. 4A). However, we observed that over a longer timescale, the separate domains compete with one another for the limited enzyme (even when “infinitely” far apart) (fig. S9), inexorably leading to the formation of a single large domain.

The spontaneous formation of a large marked domain by mark redistribution after many cell generations is reminiscent of the formation of senescence-associated heterochromatin foci (SAHF) in senescent cells, which is associated with loss of heterochromatin elsewhere (54). Present accounts of SAHF formation suggest an orchestrated process regulated by many specific effectors (55), but our findings highlight the possibility that similar behavior could be a primitive tendency of mark spreading coupled to 3D genome organization.

Longer domains are more stable against mark redistribution in direct proportion to their length (fig. S9). This effect extends to clusters of domains; as the interdomain separation is decreased, they begin to act as a single larger domain, lasting longer in competition with a larger domain (Fig. 4B). These predictions could be tested by observing the fate of artificial ectopic mark domains of differing lengths (20, 56, 57) and clusters of small marked domains.

Because tiny domains are lost quickly, mark redistribution can be viewed as a form of error correction. If “errors” appear in the form of a background rate at which monomers spontaneously switch from A to B, creating “domains” consisting of individual monomers, these errors are corrected immediately by redistribution of the marks to a larger domain (Fig. 4C and fig.

S10). Resistance to this kind of error is important for any model of epigenetic memory that is based on spreading by reader-writer enzymes because these enzymes have (at some low, but nonzero rate) nonspecific writing activity, unstimulated by the reader domain (9). Conversely, this finding suggests that mechanisms other than ours must be at work in small, unusually stable mark domains, such as the three-nucleosome *FLC* nucleation region of *Arabidopsis* (58, 59). Our model is compatible with such mechanisms; introducing small, permanently marked regions to our model does not alter the basic story (fig. S11).

Epigenetic heterogeneity can emerge stochastically and then remain stable

The final category of tests for our model stems from its ability to capture the emergence of epigenetic heterogeneity in a cell population. We considered the case in which marks are initially present in a small contiguous region and then S/L or E_T is suddenly increased (Fig. 4, D to I). This could represent a developmental event, such as an increase in the duration of the cell cycle (which effectively decreases L), or the overexpression and activation of a reader-writer enzyme (an increase in E_T). Immediately, new marks emerge randomly along the polymer, but over a few cell generations they redistribute to form one or a few large domains, strongly biased to include the small initially marked domain (Fig. 4D and movie S1). At the level of a population average (Fig. 4E), the initial domain appears to simply expand linearly into a larger one. But in fact, there is large single-cell variation involving noncontiguous domains (Fig. 4F), a prediction that single-cell epigenomic techniques (60) could test.

This behavior means that our model, without any modification or additional elements, can reproduce both classic and emerging aspects of the position-effect variegation (PEV). In PEV, translocations of the white gene of *Drosophila* to a genomic position near or within heterochromatin lead to stochastic but mitotically heritable silencing of the gene (51). This results in a variegating phenotype characterized by mottled red-white eyes, in which clonal patches bear the same coloration. Thus, the state of the locus is stochastic yet memorized over many cell divisions. To see PEV in our model, we created cell lineage trees by simply duplicating our simulation after every generation and then continuing the simulation of the copies independently. We then interrogated the marking status of a small regulatory region somewhere along the polymer to read out the silencing status over time in the lineage (Fig. 4, G to I). Solely by varying the position of this region, relative to the initially marked domain, our model reproduces drastically different observed phenotypes—including both the sectored (Fig. 4H) and “salt-and-pepper” (Fig. 4I) modes of variegation

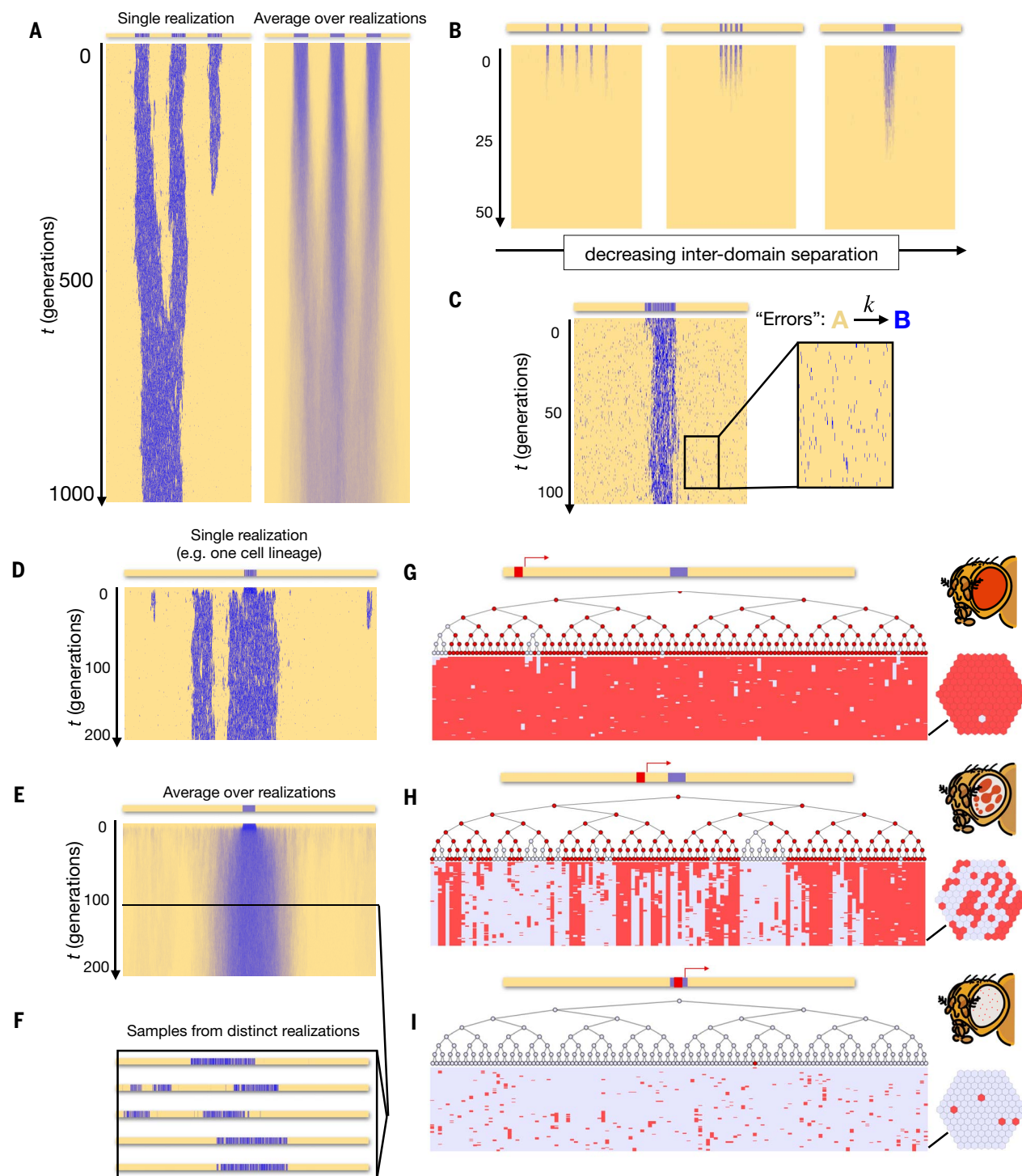
(61, 62)—thus providing a mechanistic rationale for this classic phenomenon of stochastically established yet memorized epigenetic states.

Discussion

We have shown how three ingredients—self-attraction of marked regions, 3D spread of marks, and limited enzyme—give rise to stable mark patterns that could serve as seats of epigenetic memory. Of these ingredients, we want to especially highlight the importance of the limitation of reader-writer enzymes—an element which is biologically very plausible, often neglected in models of mark dynamics, and which completely changes the system’s behavior.

The mechanism that we identified accounts for the stable maintenance of mark domains after their establishment but does not address the question of why certain regions get marked in the first place. Mark patterns can certainly be strongly influenced by processes that we do not model here, such as nucleation regions to which modifying enzymes are recruited (14, 23) or actively transcribed regions that are impervious to repressive marks (63–66). Our memory mechanism is compatible with such exogenous influences. Simulations in which we imposed the condition that some regions are “pinned” to be permanently marked (fig. S11), or conversely are unmarkable (fig. S12), exhibit stable memory of mark domains away from pinned regions. It is also possible that some genomic elements are required to license certain regions for memory (67, 68). Such conditional nucleation sites (20) could be modeled as markable regions separated by large unmarkable ones. In fact, in our model, this kind of architecture may help memory by slowing mark redistribution (fig. S12B).

Our model makes a number of assumptions and has several limitations, including its consideration of just a single epigenetic mark rather than competing or successive levels of modification, as well as the absence of attraction of heterochromatin to the nuclear lamina. We explored variants of our model that relax two of our central assumptions: the absence of mitotic mark dynamics and the absence of interphase chromatin dynamics. We found that spreading of marks during mitosis has only a small effect, most fundamentally because mitosis is short in duration relative to the length of the cell cycle (fig. S3 and supplementary text). This effect compounds (figure S3B) with any reduced activity of modifying enzymes on mitotic chromatin (e.g., due to reduced chemical or physical accessibility), further diminishing the role of possible mitotic spread of marks. Interphase dynamics can accelerate the loss of mark patterns (especially when loss is solely due to replicative dilution), but we found that this can be rescued by increasing the strength of self-attraction (fig. S4 and supplementary

**Fig. 4. Dynamics of complex patterns and position-effect variegation.**

(A) Time evolution of a pattern consisting of three equally sized mark domains ($\alpha = 2.4 k_B T$, $S/L = 0.5$, $E_T = 3000$). The pattern is stable for hundreds of generations, although marks eventually redistribute to form a single contiguous domain. In a population average (right), the three domains instead appear to merge. (B) Multiple small domains ($\alpha = 2.4 k_B T$, $S/L = 0.5$; population average shown) competing with a much bigger one (not pictured) survive redistribution longer the closer they are together. (C) Error correction: Tiny “domains” introduced by spontaneous marking at rate k are lost immediately ($\alpha = 2.4 k_B T$, $S/L = 0.5$, $E_T = 1000$, $k/L = 0.003$). (D) Expansion of marks from a small domain leads to the random formation of new domains that can be remembered for hundreds of

generations ($\alpha = 2.4 k_B T$, $S/L = 0.5$, $E_T = 3000$). (E) The population average of (D) hides the large cell variation shown in (F). (G to I) Position-effect variegation: To visualize the consequences of this, we consider a gene regulatory region of five consecutive monomers (red) somewhere along the polymer and take the presence of a single B monomer in this region to silence the gene. Investigating silencing status (white indicates silenced; red indicates not silenced) in a lineage tree generated with our model, we find different phenotypes reminiscent of the classic position-effect variegation: (G) wild-type, (H) sectored variegation, and (I) “salt-and-pepper” variegation, depending on the position of the regulatory region. [The clip art of fly eyes is from the Database Center for Life Science (CC BY 4.0).]

text). Tethering of heterochromatin to the lamina might also play this role, hinting at a mechanism that could link disruptions of the lamina to deterioration of epigenetic memory (69, 70).

A natural question to ask about epigenetic memory systems is “How much information can be stored and for how long?” As a first step toward addressing this question for our system, we chose a scheme for recording and reading out “bits” in a mark pattern and then investigated how the probability of a bit error grows over successive cell generations in our model (fig. S13 and supplementary text). We uncovered a capacity-stability tradeoff: The more bits one seeks to encode (in our polymer of fixed length), the shorter the memory. For example, our system can reliably memorize at least 8 bits for 50 generations or at least 17 bits for 20 generations. These are only lower bounds on the capacity because we have not shown that our scheme for encoding bits is optimal. Errors arise through mark redistribution, and we only poorly understand what controls the redistribution timescale, aside from the expectation that it will increase with system size. Despite these caveats, our estimate gives us a sense of scale: A mechanism such as ours (using only 10^4 monomers) could provide stability to 250 ($\sim 2^8$) alternative cellular states over 50 generations.

Intuitively, the memory mechanism that we uncovered relies on the encoding of memory in different forms in different phases of the cell cycle. In interphase, memory is held in the 3D structure of the genome in the form of density differences because dynamic marks sharply localize to dense regions. During mitosis, when the 3D structure is being totally reorganized, memory is held in the 1D sequence of marks.

The mark dynamics on a fixed polymer in our model clearly have some affinity to the protein-sequence design problem (71–73), for which the goal is to find an amino acid sequence that will fold into a target 3D structure. Classically, the design may be accomplished by choosing a sequence that minimizes the energy of the target configuration relative to all other configurations (74, 75). Analogously, our mark dynamics—although not directly minimizing the energy of a target structure—nevertheless perform a kind of sequence design, giving rise to a mark sequence that refolds into a similar polymer structure. The dynamics of our model could then be thought of as iterated rounds of design and refolding, with the goal of preserving the sequence—a problem that is different from sequence design and that to our knowledge has not been considered in the protein-folding field.

The encoding of a mark pattern through folding of the polymer, within one cell generation, could also be thought of as the “learning rule” of an associative memory in a Hopfield network (76). Learning by the Hebb rule in such networks strengthens connections between

active neurons (77, 78); here, connections between marked regions are established by folding them together (“mark together, park together”). In this analogy, the mark dynamics are like the “update rule” that allows recovery of a stored memory. This lens is particularly relevant in view of the growing recognition that single cells (79–81) and simple chemical systems (82, 83) are capable of remarkably complex behaviors and memory. The possibility that epigenetic systems are capable not just of memory but also of more sophisticated information processing, such as associative learning, should be kept in mind; it may be the key to understanding them in their full complexity.

Materials and methods

To simulate our model, we used polychrom (84), a lab-developed wrapper of OpenMM (85), for the polymer dynamics, and EoN (Epidemics on Networks) (86) for the mark dynamics. Our simulated polymer consists of 10,000 monomers connected by harmonic bonds with natural length $l = 1$. Monomers are of two types, *A* and *B*. Every pair of monomers additionally interacts according to an interparticle potential (supplementary text) that is repulsive for $r < 1$ and that for B-B pairs models short-ranged attraction between $r = 1$ and $r = 1.5$ as a smoothed square well of depth a . Finally, our polymer is confined to a sphere with radius chosen so that the volume fraction occupied by monomers is 5%. This value may be compared with a rough estimate for the volume fraction of nucleosomes in the nucleus, for example, $\sim(30 \text{ million} \times 500 \text{ nm}^3)/300 \mu\text{m}^3 = 0.05$.

In our simulations, the polymer was initialized with the “grow_cubic” function of polychrom (84), which generates a compact, unknotted random walk on cubic lattice. It was then relaxed from this state by using the variable timestep Langevin integrator of OpenMM (error tolerance = 0.00005). Note that our simulation was performed in the underdamped (ballistic) regime (frictionCoeff = 0.01 inverse OpenMM “picoseconds”) to enable use of the efficient variable timestep integrator. This did not change the equilibrium distribution of the monomer positions, from which we were interested in sampling. For all our simulations, we relaxed the polymer for 1000 OpenMM “picoseconds,” which is long enough for the polymer to expand to fill the confining sphere and to develop compartmentalization according to the monomer identities. As a control, we varied this relaxation time by a factor of 10 in either direction and observed no significant differences in the time evolution of mark patterns (fig. S15).

For the mark dynamics, we generated a contact graph, G , from the relaxed polymer configuration, where the vertices of the graph are all the monomers and there is an edge be-

tween two vertices if the distance between the associated monomers is less than the spreading radius, 1.5 (as a control, we show consequences of varying this value in fig. S16). We then simulated the dynamics of spreading and loss on this graph G with the fast_SIS (87) function of EoN, which performs an exact stochastic simulation of the Markovian SIS model on the graph G . Note that these mark dynamics are nonequilibrium (violating detailed balance).

The marks relaxed, according to their dynamics, toward an extremely long-lived metastable state from which we sought to sample (the true steady state of these dynamics is always the absorbing state where there are no marks at all). The mark relaxation time that we used in all our simulations was 200 divided by the loss rate, L , which appears more than sufficient to reach the metastable state. We tested this by varying the relaxation time in both directions and saw no appreciable changes (fig. S15).

In the case of limited enzyme, in which there is an effective spreading rate dependent on the number of marks (supplementary text), we updated the spreading rate according to the evolving number of marks 200 times for each cell generation.

REFERENCES AND NOTES

1. M. Ptashne, *A Genetic Switch: Gene Control and Phage λ* (Cell Press and Blackwell, 1986).
2. T. S. Gardner, C. R. Cantor, J. J. Collins, Construction of a genetic toggle switch in *Escherichia coli*. *Nature* **403**, 339–342 (2000). doi: [10.1038/35002131](https://doi.org/10.1038/35002131); pmid: [10659857](https://pubmed.ncbi.nlm.nih.gov/10659857/)
3. R. Zhu, J. M. Del Rio-Salgado, J. Garcia-Ojalvo, M. B. Elowitz, Synthetic multistability in mammalian cells. *Science* **375**, eabg9765 (2022). doi: [10.1126/science.abg9765](https://doi.org/10.1126/science.abg9765); pmid: [35050677](https://pubmed.ncbi.nlm.nih.gov/35050677/)
4. I. B. Dodd, M. A. Micheelsens, K. Sneppen, G. Thon, Theoretical analysis of epigenetic cell memory by nucleosome modification. *Cell* **129**, 813–822 (2007). doi: [10.1016/j.cell.2007.02.053](https://doi.org/10.1016/j.cell.2007.02.053); pmid: [17512413](https://pubmed.ncbi.nlm.nih.gov/17512413/)
5. S. Berry, M. Hartley, T. S. G. Olsson, C. Dean, M. Howard, Local chromatin recruitment of a Polycomb target gene instructs its own epigenetic inheritance. *eLife* **4**, e07205 (2015). doi: [10.7554/eLife.07205](https://doi.org/10.7554/eLife.07205); pmid: [25955967](https://pubmed.ncbi.nlm.nih.gov/25955967/)
6. I. B. Dodd, K. Sneppen, “Modeling Bistable Chromatin States” in *Epigenetics and Systems Biology* (Elsevier, 2017), pp. 145–168.
7. R. Bonasio, S. Tu, D. Reinberg, Molecular signals of epigenetic states. *Science* **330**, 612–616 (2010). doi: [10.1126/science.1191078](https://doi.org/10.1126/science.1191078); pmid: [21030644](https://pubmed.ncbi.nlm.nih.gov/21030644/)
8. R. Margueron *et al.*, Role of the polycomb protein EED in the propagation of repressive histone marks. *Nature* **461**, 762–767 (2009). doi: [10.1038/nature08398](https://doi.org/10.1038/nature08398); pmid: [19767730](https://pubmed.ncbi.nlm.nih.gov/19767730/)
9. M. M. Müller, B. Fierz, L. Bittova, G. Liszczak, T. W. Muir, A two-state activation mechanism controls the histone methyltransferase Suv39h1. *Nat. Chem. Biol.* **12**, 188–193 (2016). doi: [10.1038/nchembio.2008](https://doi.org/10.1038/nchembio.2008); pmid: [26807716](https://pubmed.ncbi.nlm.nih.gov/26807716/)
10. N. Reverón-Gómez *et al.*, Accurate recycling of parental histones reproduces the histone modification landscape during DNA replication. *Mol. Cell* **72**, 239–249.e5 (2018). doi: [10.1016/j.molcel.2018.08.010](https://doi.org/10.1016/j.molcel.2018.08.010); pmid: [30146316](https://pubmed.ncbi.nlm.nih.gov/30146316/)
11. T. M. Escobar *et al.*, Active and repressed chromatin domains exhibit distinct nucleosome segregation during DNA replication. *Cell* **179**, 953–963.e11 (2019). doi: [10.1016/j.cell.2019.10.009](https://doi.org/10.1016/j.cell.2019.10.009); pmid: [31675501](https://pubmed.ncbi.nlm.nih.gov/31675501/)
12. N. A. Hathaway *et al.*, Dynamics and memory of heterochromatin in living cells. *Cell* **149**, 1447–1460 (2012). doi: [10.1016/j.cell.2012.03.052](https://doi.org/10.1016/j.cell.2012.03.052); pmid: [22704655](https://pubmed.ncbi.nlm.nih.gov/22704655/)
13. C. Hodges, G. R. Crabtree, Dynamics of inherently bounded histone modification domains. *Proc. Natl. Acad. Sci. U.S.A.* **109**, 13296–13301 (2012). doi: [10.1073/pnas.121172109](https://doi.org/10.1073/pnas.121172109); pmid: [22847427](https://pubmed.ncbi.nlm.nih.gov/22847427/)

14. O. Oksuz *et al.*, Capturing the onset of PRC2-mediated repressive domain formation. *Mol. Cell* **70**, 1149–1162.e5 (2018). doi: [10.1016/j.molcel.2018.05.023](https://doi.org/10.1016/j.molcel.2018.05.023); pmid: [29932905](https://pubmed.ncbi.nlm.nih.gov/29932905/)
15. K. Kraft *et al.*, Polycomb-mediated genome architecture enables long-range spreading of H3K27 methylation. *Proc. Natl. Acad. Sci. U.S.A.* **119**, e2201883119 (2022). doi: [10.1073/pnas.2201883119](https://doi.org/10.1073/pnas.2201883119); pmid: [35617427](https://pubmed.ncbi.nlm.nih.gov/35617427/)
16. E. E. Dormidontova, A. Y. Grosberg, A. R. Khokhlov, Intramolecular phase separation of a copolymer chain with mobile primary structure. *Macromol. Theory Simul.* **1**, 375–385 (1992). doi: [10.1002/mats.1992040010603](https://doi.org/10.1002/mats.1992040010603)
17. D. Michieletto, E. Orlandini, D. Marenduzzo, Polymer model with epigenetic recoloring reveals a pathway for the de novo establishment and 3D organization of chromatin domains. *Phys. Rev. X* **6**, 041047 (2016). doi: [10.1103/PhysRevX.6.041047](https://doi.org/10.1103/PhysRevX.6.041047)
18. R. Cortini *et al.*, The physics of epigenetics. *Rev. Mod. Phys.* **88**, 025002 (2016). doi: [10.1103/RevModPhys.88.025002](https://doi.org/10.1103/RevModPhys.88.025002)
19. D. Jost, C. Vaillant, Epigenomics in 3D: Importance of long-range spreading and specific interactions in epigenomic maintenance. *Nucleic Acids Res.* **46**, 2252–2264 (2018). doi: [10.1093/nar/gkx009](https://doi.org/10.1093/nar/gkx009); pmid: [29365171](https://pubmed.ncbi.nlm.nih.gov/29365171/)
20. F. Erdel, E. C. Greene, Generalized nucleation and looping model for epigenetic memory of histone modifications. *Proc. Natl. Acad. Sci. U.S.A.* **113**, E4180–E4189 (2016). doi: [10.1073/pnas.1605862113](https://doi.org/10.1073/pnas.1605862113); pmid: [27382173](https://pubmed.ncbi.nlm.nih.gov/27382173/)
21. S. H. Sandholtz, Q. MacPherson, A. J. Spakowitz, Physical modeling of the heritability and maintenance of epigenetic modifications. *Proc. Natl. Acad. Sci. U.S.A.* **117**, 20423–20429 (2020). doi: [10.1073/pnas.1920499117](https://doi.org/10.1073/pnas.1920499117); pmid: [32778583](https://pubmed.ncbi.nlm.nih.gov/32778583/)
22. M. Katava, G. Shi, D. Thirumalai, Chromatin dynamics controls epigenetic domain formation. *Biophys. J.* **121**, 2895–2905 (2022). doi: [10.1016/j.bpj.2022.07.001](https://doi.org/10.1016/j.bpj.2022.07.001); pmid: [35799447](https://pubmed.ncbi.nlm.nih.gov/35799447/)
23. D. Michieletto *et al.*, Shaping epigenetic memory via genomic bookmarking. *Nucleic Acids Res.* **46**, 83–93 (2018). doi: [10.1093/nar/gkx1200](https://doi.org/10.1093/nar/gkx1200); pmid: [29190361](https://pubmed.ncbi.nlm.nih.gov/29190361/)
24. A. Z. Abdulla, C. Vaillant, D. Jost, Painters in chromatin: A unified quantitative framework to systematically characterize epigenome regulation and memory. *Nucleic Acids Res.* **50**, 9083–9104 (2022). doi: [10.1093/nar/gkac702](https://doi.org/10.1093/nar/gkac702); pmid: [36018799](https://pubmed.ncbi.nlm.nih.gov/36018799/)
25. H. Bauer, Structure and arrangement of salivary gland chromosomes in Drosophila species. *Proc. Natl. Acad. Sci. U.S.A.* **22**, 216–222 (1936). doi: [10.1073/pnas.22.4.216](https://doi.org/10.1073/pnas.22.4.216); pmid: [16577698](https://pubmed.ncbi.nlm.nih.gov/16577698/)
26. A. R. Strom *et al.*, Phase separation drives heterochromatin domain formation. *Nature* **547**, 241–245 (2017). doi: [10.1038/nature22989](https://doi.org/10.1038/nature22989); pmid: [28636597](https://pubmed.ncbi.nlm.nih.gov/28636597/)
27. A. G. Larson *et al.*, Liquid droplet formation by HP1α suggests a role for phase separation in heterochromatin. *Nature* **547**, 236–240 (2017). doi: [10.1038/nature22822](https://doi.org/10.1038/nature22822); pmid: [28636604](https://pubmed.ncbi.nlm.nih.gov/28636604/)
28. M. Falk *et al.*, Heterochromatin drives compartmentalization of inverted and conventional nuclei. *Nature* **570**, 395–399 (2019). doi: [10.1038/s41586-019-1275-3](https://doi.org/10.1038/s41586-019-1275-3); pmid: [31168090](https://pubmed.ncbi.nlm.nih.gov/31168090/)
29. H. Strickfaden, A. Zunhammer, S. van Koningsbruggen, D. Köhler, T. Cremer, 4D chromatin dynamics in cycling cells: Theodor Boveri's hypotheses revisited. *Nucleus* **1**, 284–297 (2010). doi: [10.4161/nucl.11969](https://doi.org/10.4161/nucl.11969); pmid: [21327076](https://pubmed.ncbi.nlm.nih.gov/21327076/)
30. C. Kadoc *et al.*, Dynamics of BAF-Polycomb complex opposition on heterochromatin in normal and oncogenic states. *Nat. Genet.* **49**, 213–222 (2017). doi: [10.1038/ng.3734](https://doi.org/10.1038/ng.3734); pmid: [27941796](https://pubmed.ncbi.nlm.nih.gov/27941796/)
31. P. Dobrinić, A. T. Szczurek, R. J. Klose, PRC1 drives Polycomb-mediated gene repression by controlling transcription initiation and burst frequency. *Nat. Struct. Mol. Biol.* **28**, 811–824 (2021). doi: [10.1038/s41594-021-00661-y](https://doi.org/10.1038/s41594-021-00661-y); pmid: [34608337](https://pubmed.ncbi.nlm.nih.gov/34608337/)
32. M. Gabriele *et al.*, Dynamics of CTCF- and cohesin-mediated chromatin looping revealed by live-cell imaging. *Science* **376**, 496–501 (2022). doi: [10.1126/science.abn6583](https://doi.org/10.1126/science.abn6583); pmid: [35420890](https://pubmed.ncbi.nlm.nih.gov/35420890/)
33. K. Ito, K. S. Zaret, Maintaining transcriptional specificity through mitosis. *Annu. Rev. Genomics Hum. Genet.* **23**, 53–71 (2022). doi: [10.1146/annurev-genom-121321-094603](https://doi.org/10.1146/annurev-genom-121321-094603); pmid: [35440147](https://pubmed.ncbi.nlm.nih.gov/35440147/)
34. Y. Liu *et al.*, Widespread mitotic bookmarking by histone marks and transcription factors in pluripotent stem cells. *Cell Rep.* **19**, 1283–1293 (2017). doi: [10.1016/j.celrep.2017.04.067](https://doi.org/10.1016/j.celrep.2017.04.067); pmid: [28514649](https://pubmed.ncbi.nlm.nih.gov/28514649/)
35. S. Rea *et al.*, Regulation of chromatin structure by site-specific histone H3 methyltransferases. *Nature* **406**, 593–599 (2000). doi: [10.1038/35020506](https://doi.org/10.1038/35020506); pmid: [10949293](https://pubmed.ncbi.nlm.nih.gov/10949293/)
36. P. N. I. Lau, P. Cheung, Histone code pathway involving H3 S28 phosphorylation and K27 acetylation activates transcription and antagonizes Polycomb silencing. *Proc. Natl. Acad. Sci. U.S.A.* **108**, 2801–2806 (2011). doi: [10.1073/pnas.1012798108](https://doi.org/10.1073/pnas.1012798108); pmid: [21282660](https://pubmed.ncbi.nlm.nih.gov/21282660/)
37. R. Pastor-Satorras, C. Castellano, P. Van Mieghem, A. Vespignani, Epidemic processes in complex networks. *Rev. Mod. Phys.* **87**, 925–979 (2015). doi: [10.1103/RevModPhys.87.925](https://doi.org/10.1103/RevModPhys.87.925)
38. J. M. Stafford *et al.*, Multiple modes of PRC2 inhibition elicit global chromatin alterations in H3K27M pediatric glioma. *Sci. Adv.* **4**, eaau5935 (2018). doi: [10.1126/sciadv.aau5935](https://doi.org/10.1126/sciadv.aau5935); pmid: [30420543](https://pubmed.ncbi.nlm.nih.gov/30420543/)
39. R. Leicher *et al.*, Single-molecule and *in silico* dissection of the interaction between Polycomb repressive complex 2 and chromatin. *Proc. Natl. Acad. Sci. U.S.A.* **117**, 30465–30475 (2020). doi: [10.1073/pnas.200395117](https://doi.org/10.1073/pnas.200395117); pmid: [3208532](https://pubmed.ncbi.nlm.nih.gov/3208532/)
40. M. A. Gillespie *et al.*, Absolute Quantification of Transcription Factors Reveals Principles of Gene Regulation in Erythropoiesis. *Mol. Cell* **78**, 960–974.e11 (2020). doi: [10.1016/j.molcel.2020.03.031](https://doi.org/10.1016/j.molcel.2020.03.031); pmid: [32330456](https://pubmed.ncbi.nlm.nih.gov/32330456/)
41. L. Michaelis, M. L. Menten, K. A. Johnson, R. S. Goody, The original Michaelis constant: Translation of the 1913 Michaelis-Menten paper. *Biochemistry* **50**, 8264–8269 (2011). doi: [10.1021/bi01284u](https://doi.org/10.1021/bi01284u); pmid: [21888353](https://pubmed.ncbi.nlm.nih.gov/21888353/)
42. J. Gunawardena, Time-scale separation—Michaelis and Menten's old idea, still bearing fruit. *FEBS J.* **281**, 473–488 (2014). doi: [10.1111/febs.12532](https://doi.org/10.1111/febs.12532); pmid: [24103070](https://pubmed.ncbi.nlm.nih.gov/24103070/)
43. A. Bancaud *et al.*, Molecular crowding affects diffusion and binding of nuclear proteins in heterochromatin and reveals the fractal organization of chromatin. *EMBO J.* **28**, 3785–3798 (2009). doi: [10.1038/embj.2009.340](https://doi.org/10.1038/embj.2009.340); pmid: [19927119](https://pubmed.ncbi.nlm.nih.gov/19927119/)
44. M. T. McCabe *et al.*, EZH2 inhibition as a therapeutic strategy for lymphoma with EZH2-activating mutations. *Nature* **492**, 108–112 (2012). doi: [10.1038/nature11606](https://doi.org/10.1038/nature11606); pmid: [23051747](https://pubmed.ncbi.nlm.nih.gov/23051747/)
45. W. Béguelin *et al.*, Mutant EZH2 induces a pre-malignant lymphoma niche by reprogramming the immune response. *Cancer Cell* **37**, 655–673.e11 (2020). doi: [10.1016/j.ccr.2020.04.004](https://doi.org/10.1016/j.ccr.2020.04.004); pmid: [32396861](https://pubmed.ncbi.nlm.nih.gov/32396861/)
46. G. P. Souroullas *et al.*, An oncogenic Ezh2 mutation induces tumors through global redistribution of histone 3 lysine 27 trimethylation. *Nat. Med.* **22**, 632–640 (2016). doi: [10.1038/nm.4092](https://doi.org/10.1038/nm.4092); pmid: [27135738](https://pubmed.ncbi.nlm.nih.gov/27135738/)
47. K. L. Diehl *et al.*, PRC2 engages a bivalent H3K27M-H3K27me3 dinucleosome inhibitor. *Proc. Natl. Acad. Sci. U.S.A.* **116**, 22152–22157 (2019). doi: [10.1073/pnas.1911775116](https://doi.org/10.1073/pnas.1911775116); pmid: [31611394](https://pubmed.ncbi.nlm.nih.gov/31611394/)
48. H. D. Ou *et al.*, ChromEMT: Visualizing 3D chromatin structure and compaction in interphase and mitotic cells. *Science* **357**, eaag0025 (2017). doi: [10.1126/science.aag0025](https://doi.org/10.1126/science.aag0025); pmid: [28751582](https://pubmed.ncbi.nlm.nih.gov/28751582/)
49. S. Murphy, A. N. Boettiger, Polycomb repression of Hox genes involves spatial feedback but not domain compaction or demixing. *bioRxiv* 2022.10.14.512199 [Preprint] (2022). doi: [10.1101/2022.10.14.512199](https://doi.org/10.1101/2022.10.14.512199).
50. C. Alabert *et al.*, Two distinct modes for propagation of histone PTMs across the cell cycle. *Genes Dev.* **29**, 585–590 (2015). doi: [10.1101/gad.256354.114](https://doi.org/10.1101/gad.256354.114); pmid: [25792596](https://pubmed.ncbi.nlm.nih.gov/25792596/)
51. S. C. R. Elgin, G. Reuter, Position-effect variegation, heterochromatin formation, and gene silencing in Drosophila. *Cold Spring Harb. Perspect. Biol.* **5**, a017780 (2013). doi: [10.1101/cshperspect.a017780](https://doi.org/10.1101/cshperspect.a017780); pmid: [23906716](https://pubmed.ncbi.nlm.nih.gov/23906716/)
52. C. M. Weber *et al.*, mSWI/SNF promotes Polycomb repression both directly and through genome-wide redistribution. *Nat. Struct. Mol. Biol.* **28**, 501–511 (2021). doi: [10.1038/s41594-021-00604-7](https://doi.org/10.1038/s41594-021-00604-7); pmid: [34117481](https://pubmed.ncbi.nlm.nih.gov/34117481/)
53. E. Conway *et al.*, BAP1 enhances Polycomb repression by counteracting widespread H2AK119ub1 deposition and chromatin condensation. *Mol. Cell* **81**, 3526–3541.e8 (2021). doi: [10.1016/j.molcel.2020.116.020](https://doi.org/10.1016/j.molcel.2020.116.020); pmid: [34186021](https://pubmed.ncbi.nlm.nih.gov/34186021/)
54. X. Zhang *et al.*, The loss of heterochromatin is associated with multiscale three-dimensional genome reorganization and aberrant transcription during cellular senescence. *Genome Res.* **31**, 1121–1135 (2021). doi: [10.1101/gr.275251.121](https://doi.org/10.1101/gr.275251.121); pmid: [34140314](https://pubmed.ncbi.nlm.nih.gov/34140314/)
55. I. Olan, M. Narita, Senescence: An Identity Crisis Originating from Deep Within the Nucleus. *Annu. Rev. Cell Dev. Biol.* **38**, 219–239 (2022). doi: [10.1146/annurev-genom-121321-094603](https://doi.org/10.1146/annurev-genom-121321-094603); pmid: [35440147](https://pubmed.ncbi.nlm.nih.gov/35440147/)
56. P. I. Thakore *et al.*, Highly specific epigenome editing by CRISPR-Cas9 repressors for silencing of distal regulatory elements. *Nat. Methods* **12**, 1143–1149 (2015). doi: [10.1038/nmeth.3630](https://doi.org/10.1038/nmeth.3630); pmid: [26501517](https://pubmed.ncbi.nlm.nih.gov/26501517/)
57. J. Pulecio, N. Verma, E. Mejia-Ramirez, D. Huangfu, A. Ray, CRISPR/Cas9-based engineering of the epigenome. *Cell Stem Cell* **21**, 431–447 (2017). doi: [10.1016/j.stem.2017.09.006](https://doi.org/10.1016/j.stem.2017.09.006); pmid: [28985525](https://pubmed.ncbi.nlm.nih.gov/28985525/)
58. H. Yang *et al.*, Distinct phases of Polycomb silencing to hold epigenetic memory of cold in *Arabidopsis*. *Science* **357**, 1142–1145 (2017). doi: [10.1126/science.aan1121](https://doi.org/10.1126/science.aan1121); pmid: [28818969](https://pubmed.ncbi.nlm.nih.gov/28818969/)
59. C. Lövkist *et al.*, Hybrid protein assembly-histone modification mechanism for PRC2-based epigenetic switching and memory. *eLife* **10**, e66454 (2021). doi: [10.7554/eLife.66454](https://doi.org/10.7554/eLife.66454); pmid: [34473050](https://pubmed.ncbi.nlm.nih.gov/34473050/)
60. S. Preissl, K. J. Gaulton, B. Ren, Characterizing *cis*-regulatory elements using single-cell epigenomics. *Nat. Rev. Genet.* **24**, 21–43 (2022). doi: [10.1038/s41576-022-00509-1](https://doi.org/10.1038/s41576-022-00509-1); pmid: [35840754](https://pubmed.ncbi.nlm.nih.gov/35840754/)
61. B. Y. Lu, C. P. Bishop, J. C. Eisenberg, Developmental timing and tissue specificity of heterochromatin-mediated silencing. *EMBO J.* **15**, 1323–1332 (1996). doi: [10.1002/j.1460-205.1996.tb00474.x](https://doi.org/10.1002/j.1460-205.1996.tb00474.x); pmid: [8635465](https://pubmed.ncbi.nlm.nih.gov/8635465/)
62. F. Buglio, G. R. Huckell, K. A. Maggert, Monitoring of switches in heterochromatin-induced silencing shows incomplete establishment and developmental instabilities. *Proc. Natl. Acad. Sci. U.S.A.* **116**, 20043–20053 (2019). doi: [10.1073/pnas.1909724116](https://doi.org/10.1073/pnas.1909724116); pmid: [31527269](https://pubmed.ncbi.nlm.nih.gov/31527269/)
63. F. W. Schmitz *et al.*, Histone methylation by PRC2 is inhibited by active chromatin marks. *Mol. Cell* **42**, 330–341 (2011). doi: [10.1016/j.molcel.2011.03.025](https://doi.org/10.1016/j.molcel.2011.03.025); pmid: [21549310](https://pubmed.ncbi.nlm.nih.gov/21549310/)
64. S. Henikoff, A. Shilatifard, Histone modification: Cause or cog? *Trends Genet.* **27**, 389–396 (2011). doi: [10.1016/j.tig.2011.06.006](https://doi.org/10.1016/j.tig.2011.06.006); pmid: [21764166](https://pubmed.ncbi.nlm.nih.gov/21764166/)
65. S. Berry, C. Dean, M. Howard, Slow chromatin dynamics allow polycomb target genes to filter fluctuations in transcription factor activity. *Cell Syst.* **4**, 445–457.e8 (2017). doi: [10.1016/j.cels.2017.02.013](https://doi.org/10.1016/j.cels.2017.02.013); pmid: [28342717](https://pubmed.ncbi.nlm.nih.gov/28342717/)
66. C. Lövkist, M. Howard, Using computational modelling to reveal mechanisms of epigenetic Polycomb control. *Biochem. Soc. Trans.* **49**, 71–77 (2021). doi: [10.1042/BST20190955](https://doi.org/10.1042/BST20190955); pmid: [33616630](https://pubmed.ncbi.nlm.nih.gov/33616630/)
67. R. T. Coleman, G. Struhl, Causal role for inheritance of H3K27me3 in maintaining the OFF state of a *Drosophila* HOX gene. *Science* **356**, eaai8236 (2017). doi: [10.1126/science.aai8236](https://doi.org/10.1126/science.aai8236); pmid: [28302795](https://pubmed.ncbi.nlm.nih.gov/28302795/)
68. T. A. Shafiq, D. Moazed, Three rules for epigenetic inheritance of human Polycomb silencing. *bioRxiv* 2023.02.27.530239 [Preprint] (2023). doi: [10.1101/2023.02.27.530239](https://doi.org/10.1101/2023.02.27.530239)
69. D. K. Shumaker *et al.*, Mutant nuclear lamin A leads to progressive alterations of epigenetic control in premature aging. *Proc. Natl. Acad. Sci. U.S.A.* **103**, 8703–8708 (2006). doi: [10.1073/pnas.0602569103](https://doi.org/10.1073/pnas.0602569103); pmid: [16738054](https://pubmed.ncbi.nlm.nih.gov/16738054/)
70. A. Karoutas, A. Akhtar, Functional mechanisms and abnormalities of the nuclear lamina. *Nat. Cell Biol.* **23**, 116–126 (2021). doi: [10.1038/s41556-020-00630-5](https://doi.org/10.1038/s41556-020-00630-5); pmid: [33558730](https://pubmed.ncbi.nlm.nih.gov/33558730/)
71. V. S. Pande, A. Y. Grosberg, T. Tanaka, Heteropolymer freezing and design: Towards physical models of protein folding. *Rev. Mod. Phys.* **72**, 259–314 (2000). doi: [10.1103/RevModPhys.72.259](https://doi.org/10.1103/RevModPhys.72.259)
72. A. Y. Grosberg, A. R. Khokhlov, Giant Molecules: Here, There, and Everywhere (World Scientific Publishing, ed. 2, 2010).
73. T. M. Fink, R. C. Ball, How many conformations can a protein remember? *Phys. Rev. Lett.* **87**, 198103 (2001). doi: [10.1103/PhysRevLett.87.198103](https://doi.org/10.1103/PhysRevLett.87.198103); pmid: [11690459](https://pubmed.ncbi.nlm.nih.gov/11690459/)
74. E. I. Shakhnovich, A. M. Gutin, Engineering of stable and fast-folding sequences of model proteins. *Proc. Natl. Acad. Sci. U.S.A.* **90**, 7195–7199 (1993). doi: [10.1073/pnas.90.15.7195](https://doi.org/10.1073/pnas.90.15.7195); pmid: [8346235](https://pubmed.ncbi.nlm.nih.gov/8346235/)
75. V. S. Pande, A. Y. Grosberg, T. Tanaka, Thermodynamic procedure to synthesize heteropolymers that can renature to recognize a given target molecule. *Proc. Natl. Acad. Sci. U.S.A.* **91**, 12976–12979 (1994). doi: [10.1073/pnas.91.26.12976](https://doi.org/10.1073/pnas.91.26.12976); pmid: [7809158](https://pubmed.ncbi.nlm.nih.gov/7809158/)
76. J. J. Hopfield, Neural networks and physical systems with emergent collective computational abilities. *Proc. Natl. Acad. Sci. U.S.A.* **79**, 2554–2558 (1982). doi: [10.1073/pnas.79.8.2554](https://doi.org/10.1073/pnas.79.8.2554); pmid: [6953413](https://pubmed.ncbi.nlm.nih.gov/6953413/)
77. D. O. Hebb, *The Organization of Behavior: A Neuropsychological Theory* (Wiley, 1949).
78. S. Löwel, W. Singer, Selection of intrinsic horizontal connections in the visual cortex by correlated neuronal activity. *Science* **255**, 209–212 (1992). doi: [10.1126/science.1372754](https://doi.org/10.1126/science.1372754); pmid: [1372754](https://pubmed.ncbi.nlm.nih.gov/1372754/)
79. J. P. Dexter, S. Prabakaran, J. Gunawardena, A complex hierarchy of avoidance behaviors in a single-cell eukaryote. *Curr. Biol.* **29**, 4323–4329.e2 (2019). doi: [10.1016/j.cub.2019.10.059](https://doi.org/10.1016/j.cub.2019.10.059); pmid: [31813604](https://pubmed.ncbi.nlm.nih.gov/31813604/)
80. S. J. Gershman, P. E. M. Balbi, C. R. Gallistel, J. Gunawardena, Reconsidering the evidence for learning in single cells. *eLife* **10**, e61907 (2021). doi: [10.7554/eLife.61907](https://doi.org/10.7554/eLife.61907); pmid: [33395388](https://pubmed.ncbi.nlm.nih.gov/33395388/)

81. M. Kramar, K. Alim, Encoding memory in tube diameter hierarchy of living flow network. *Proc. Natl. Acad. Sci. U.S.A.* **118**, e2007815118 (2021). doi: [10.1073/pnas.2007815118](https://doi.org/10.1073/pnas.2007815118); pmid: [33619174](#)
82. A. Murugan, Z. Zeravcic, M. P. Brenner, S. Leibler, Multifarious assembly mixtures: Systems allowing retrieval of diverse stored structures. *Proc. Natl. Acad. Sci. U.S.A.* **112**, 54–59 (2015). doi: [10.1073/pnas.1413941112](https://doi.org/10.1073/pnas.1413941112); pmid: [25535383](#)
83. W. Zhong, D. J. Schwab, A. Murugan, Associative pattern recognition through macro-molecular self-assembly. *J. Stat. Phys.* **167**, 806–826 (2017). doi: [10.1007/s10955-017-1774-2](https://doi.org/10.1007/s10955-017-1774-2)
84. M. Imakaev, A. Goloborodko, H. B. Brandão, mirnylab/polychrom: v0.1.0, Zenodo (2019); <https://doi.org/10.5281/ZENODO.3579473>.
85. P. Eastman *et al.*, OpenMM 7: Rapid development of high performance algorithms for molecular dynamics. *PLOS Comput. Biol.* **13**, e1005659 (2017). doi: [10.1371/journal.pcbi.1005659](https://doi.org/10.1371/journal.pcbi.1005659); pmid: [28746339](#)
86. J. C. Miller, T. Ting, EoN (Epidemics on Networks): A fast, flexible Python package for simulation, analytic approximation, and analysis of epidemics on networks. *J. Open Source Softw.* **4**, 1731 (2019). doi: [10.21105/joss.01731](https://doi.org/10.21105/joss.01731)
87. I. Z. Kiss, J. C. Miller, P. L. Simon, *Mathematics of Epidemics on Networks: From Exact to Approximate Models* (Springer, 2017).
88. J. Owen, jaowen/3d-epigenetic-memory: First release, Version v1, Zenodo (2023); <https://dx.doi.org/10.5281/ZENODO.8322781>.

ACKNOWLEDGMENTS

The authors are very grateful to M. Kardar for valuable scientific discussions. **Funding:** This research was funded by the National Human Genome Research Institute, NIH grant 3UM1HG011536 (L.M.); the National Institute of General Medical Sciences, NIH grant GM114190 (L.M.); and NSF award 2044895 (L.M.). **Author contributions:** Conceptualization: J.A.O., D.O., and L.M. Methodology: J.A.O., D.O., and L.M. Investigation: J.A.O., D.O., and L.M. Funding acquisition: L.M. Project administration: L.M. Supervision: L.M. Writing – original draft: J.A.O., D.O., and L.M. Writing – review and editing: J.A.O., D.O., and L.M. **Competing**

interests: The authors declare that they have no competing interests. **Data and materials availability:** To simulate our model, we used polychrom (84), a lab-developed wrapper of OpenMM (85) for the polymer dynamics, and EoN (Epidemics on Networks) (86) for the mark dynamics. Code is available at <https://github.com/jaowen/3d-epigenetic-memory/> and deposited at Zenodo (88).

License information: Copyright © 2023 the authors; some rights reserved; exclusive licensee American Association for the Advancement of Science. No claim to original US government works. <https://www.science.org/about/science-licenses-journal-article-reuse>

SUPPLEMENTARY MATERIALS

science.org/doi/10.1126/science.adg3053

Supplementary Text

Figs. S1 to S16

References (89–94)

Movie S1

Submitted 14 December 2022; accepted 28 September 2023
10.1126/science.adg3053